

Lineage optimization in nematode's early embryogenesis

Guoye Guan,¹ Ming-Kin Wong,² Zhongying Zhao,^{2,3} Lei-Han Tang,^{4,5,*} and Chao Tang^{1,6,7,*}

¹ Center for Quantitative Biology, Peking University, Beijing 100871, China

² Department of Biology, Hong Kong Baptist University, Hong Kong 999077, China

³ State Key Laboratory of Environmental and Biological Analysis, Hong Kong Baptist University, Hong Kong 999077, China

⁴ Department of Physics, Hong Kong Baptist University, Hong Kong 999077, China

⁵ Institute of Computational and Theoretical Studies, Hong Kong Baptist University, Hong Kong 999077, China

⁶ Peking-Tsinghua Center for Life Sciences, Peking University, Beijing 100871, China

⁷ School of Physics, Peking University, Beijing 100871, China

* To whom correspondence should be addressed. Email: lhtang@hkbu.edu.hk or tangc@pku.edu.cn.

Nematode species are well-known for their invariant cell lineage pattern, including reproducible division timing, volume segregation, fate specification and migration trajectory for each and every cell during embryonic development. Here, we study the fundamental principle optimizing cell lineage pattern with *Caenorhabditis elegans*. Combining previous knowledge about the fate specification induced by asymmetric division and the anti-correlation between cell cycle length and cell volume, we propose a model to simulate lineage by altering cell volume segregation ratio in each division, and quantify the derived lineage's performance in proliferation rapidity, fate diversity and space robustness (PFS Model). The stereotypic pattern in early *C. elegans* embryo is one of the most optimal solutions taking minimum time to achieve the cell number before gastrulation. Our methods lay a foundation for deciphering principles of development and guiding designs of bio-system.

INTRODUCTION

Metazoan embryogenesis starts from a fertilized zygote and ends into numerous cells with multiple fates and structural organizations. This dynamic process needs elaborate coordination on cell behaviors at both genetic and physical levels [1-4]. In eutelic nematode *C. elegans*, the developmental programs are accurate at cellular level and invariant among individual embryos [Figs. 1(a)-1(b)] [5], which have been documented systematically by high-resolution microscopes and automatic tracing software [6-9]. The cell divisions before maternal-zygotic transition and gastrulation onset (i.e., from 1- to 24-cell stage) are ordered in a distinct sequence, which was previously proposed to ensure precise and robust cell movement [9-13]. These programed cell divisions are asymmetric in germline stem cells P0, P1, P2 and P3, and symmetric in somatic lineages AB, EMS and C [Figs. 1(b)-1(c)]. The consecutive asymmetric segregations of cell volume and its molecular contents in P cells are driven by cell polarization, and keep generating new somatic lineages with different fates [14-15]. Recently, several works uncovered an anti-correlation between cell cycle and cell volume, and suggested that these developmental properties, i.e. cell movement, cell cycle, cell volume and cell fate, are well coordinated during *C. elegans* early embryogenesis [12-13,16-17].

The anti-correlation between cell cycle length and cell volume directly influences temporal ordering of descendent cells under asymmetric cell division, and therefore sets an important physical constraint on optimizing the developmental program in a confined space. In this work, we simulate and analyze lineages controlled by cell volume segregation ratios using an empirical power-law that encodes the anti-correlation. We evaluate each lineage's performance in terms of its proliferation rapidity, fate diversity and space robustness, and find a minimum time principle governing the cell lineage pattern observed *in vivo*.

METHODS

Figure 1(a) shows images from a typical dataset of *C. elegans* embryonic development *in vivo*, which forms the basis of our model study (Supplemental Material 1). The temporal sequence of successive cell divisions defines a cell lineage pattern such as the one shown in Fig. 1(b). We assign an index i to a cell based on its division timing in the sequence, e.g., P0 cell has an index 1, AB cell has an index 2, etc. The volume segregation ratio in the division of cell i is denoted by η_i , the volume ratio between its daughters ($\eta_i \geq 1$). Besides, the i^{th} cell's volume, cycle length and division timing are denoted by V_i , T_i and t_i respectively. Then, based on the experimental data produced in our previous works [8-9], two assumptions are introduced in the construction of our lineage model.

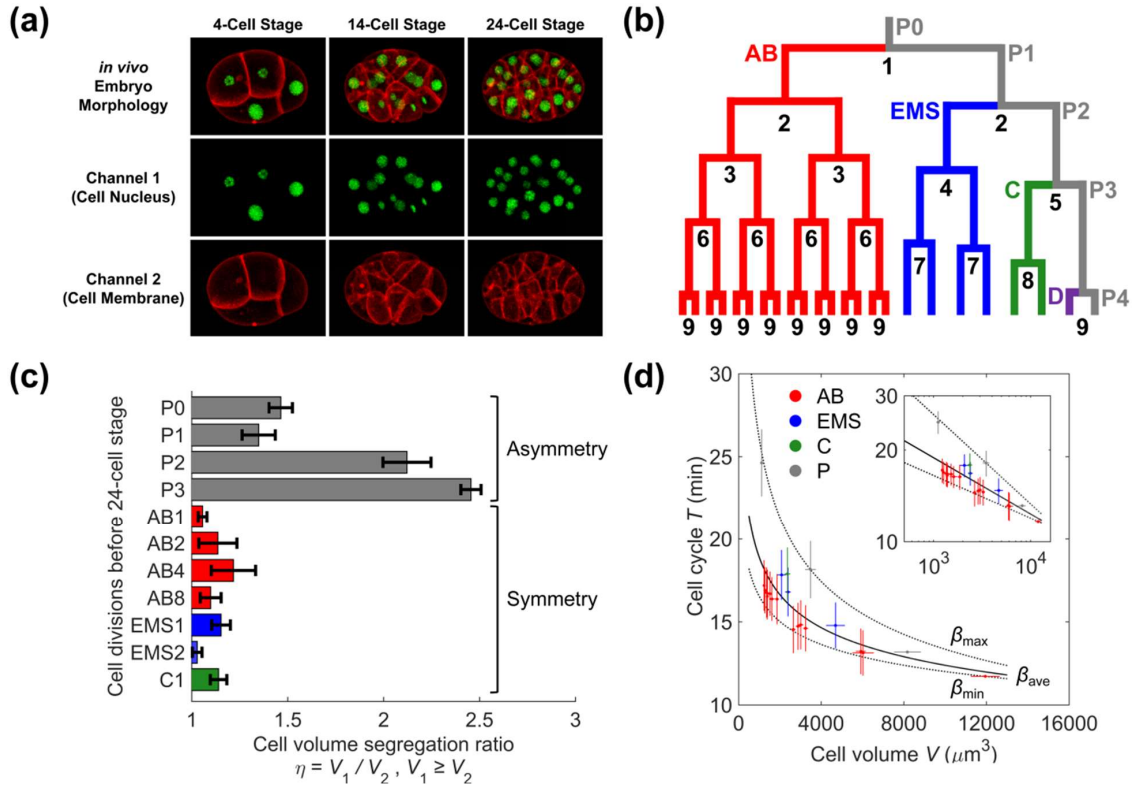


FIG. 1. *C. elegans* embryogenesis up to 24-cell stage. (a) *In vivo* *C. elegans* embryo morphology illustrated with fluorescence on cell nucleus (GFP) and cell membrane (mCherry). (b) Lineage tree with invariant division order and fate specificity. (c) Cell volume segregation ratio; error bar, standard deviation. (d) Anti-correlation between cell cycle and cell volume, together with fitted power law function Eq. (2); inset, data shown on logarithmic scale.

First, we introduce a division asymmetry threshold η_c in the fate determination of daughter cells. Two daughter cells are assigned different fate when the volume segregation ratio of their mother exceeds the threshold, i.e. $\eta > \eta_c$. The value of η_c is chosen to be 1.28, the average of maximum ratio in symmetric divisions and minimum ratio in asymmetric divisions acquired by experiments [Figs. 1(b)-1(c)] [8]. Then, we use a ternary-valued code $\{f\} = [f_1, f_2, \dots, f_I]$ to represent and trace the fate specification history of a given cell according to Eq. (1). Here, $\{I\}$ labels the cell's ancestry in descending order; $f = 0$ denotes daughters generated by symmetric division; $f = -1$ and $f = 1$ denote the smaller and larger daughters generated by asymmetric division [Fig. 2]. For example, the AB, EMS, C and P3 cells are coded with $[1]$, $[-1, 1]$, $[-1, -1, 1]$ and $[-1, -1, -1]$ respectively.

$$\{f\} = [f_1, f_2, \dots, f_I], f = \begin{cases} 0 & \eta \leq \eta_c \\ -1 & \text{smaller daughter, } \eta > \eta_c \\ 1 & \text{larger daughter, } \eta > \eta_c \end{cases} \quad (1)$$

Second, we quantify the anti-correlation between cell cycle and cell volume with a general power law in Eq. (2) [Fig. 1(d)] [16]. This global rule is attributed to the degradation and distribution of machinery proteins over cell proliferation before maternal-zygotic transition [17-18]. The actual relationship varies to some extent between cells and between lineages caused by a number of factors, such as the mitosis duration from prophase to anaphase and the initial contents of machinery proteins ($\beta_{\min} = 0.14$, $\beta_{\text{ave}} = 0.18$, $\beta_{\max} = 0.29$) [Fig. 1(d)]. Nevertheless, simulations and further analysis demonstrate that our main conclusions still hold over a change of the specific function forms or parameter settings (Supplemental Material 2).

$$T = T_1(V/V_1)^{-\beta} \quad (2)$$

Regarding the assumptions above, a given sequence of cell volume segregation ratio $\{\eta_i\}$ determines fate specifications by Eq. (1) and division timings by Eq. (2), constructing a certain cell lineage pattern. Next, we evaluate three developmental performances of a given lineage, including proliferation rapidity, fate diversity and space robustness (PFS Model).

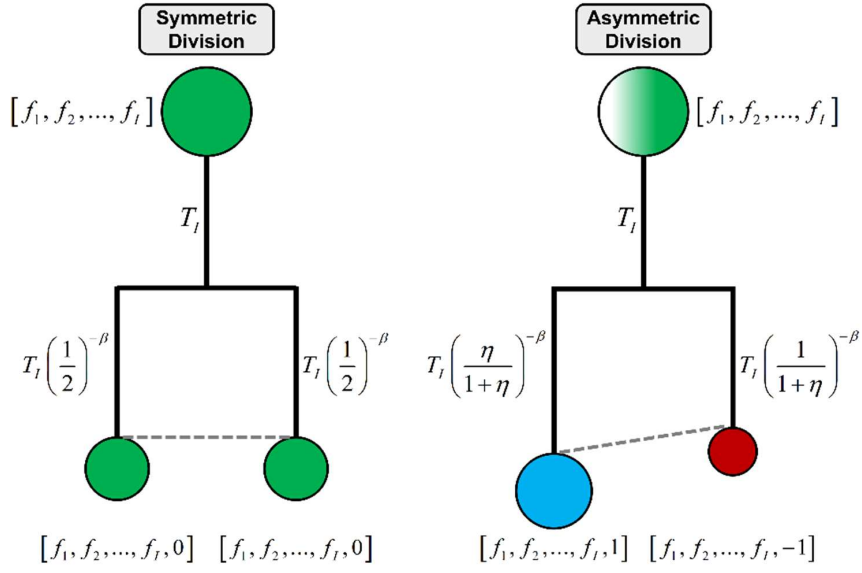


FIG. 2. Cell fate specification and cell division timing under control of Eqs. (1)-(2). Left, symmetric division with $\eta = 1$; right, asymmetric division with $\eta > \eta_c$.

Proliferation Rapidity. We use the reciprocal of total duration taken to reach a target cell number N as a lineage's proliferation rapidity, given by Eq. (3) [19].

$$P = 1/t_{N-1} \quad (3)$$

Fate Diversity. We count the non-identical fate codes among the cells at the last second round of divisions before N -cell stage [Eq. (4)]. The last round of divisions are excluded because their segregation ratios have no effect on the final division timing t_{N-1} or the proliferation rapidity P [Eq. (3)]. Note that other fate-inducing mechanisms without significant influence on cell volume segregation ratio (e.g., Wnt and Notch signaling) is not considered here [20-21].

$$F = \text{Count}\{\{f\} | \text{the last } 2^{\text{nd}} \text{ round of divisions}\} \quad (4)$$

Space Robustness. Cell divisions that take place either synchronously (to enable simultaneous collective motion) or asynchronously (to allow independent relaxation) have been shown to be essential for preserving spatial organization of a developing embryo [12-13]. For a given set of cell division times $\{t_i\}$, one may identify clusters of division events that fall within a time interval δ_s , and isolated ones at a time interval δ_a or longer from the neighboring divisions. The ones beyond these fail-safe clusters or isolated events are regarded as unstable and harmful. Therefore, we choose the number of intervals that obey these two rules to represent space robustness ($S \leq N-2$).

$$S = \text{Count}\{t_{i+n} - t_i < \delta_s\} + \text{Count}\{t_{i+1} - t_i > \delta_a\} \quad (5)$$

For *C. elegans* early embryo, the system parameters abovementioned are obtained or fitted from *in vivo* data: $\eta_c = 1.28$, $V_1 = 2.01 \times 10^4 \mu\text{m}^3$, $T_1 = 10.90 \text{ min}$, $\beta_{\text{ave}} = 0.18$, $N = 24$, $\delta_s = 1.5 \text{ min}$, $\delta_a = 3.0 \text{ min}$ [8-9].

Next, we sample the independent variables $\{\eta_i\}$ and derive the corresponding sequences of cell division timing $\{t_i\}$ according to Eq. (2). We use a modified normal distribution Eq. (6) for assigning random values to $\{\eta_i\}$, where $\eta_{\text{max}} = 3.21$ is the maximum cell volume segregation ratio detected among the first seven generations of cells in experiment, and $\text{Norm}(\eta_{\text{max}}/2, \eta_{\text{max}}/2)$ denotes a normal distribution with center at $\eta_{\text{max}}/2$ and standard deviation of $\eta_{\text{max}}/2$.

$$\eta_i = \begin{cases} \text{Norm}(\eta_{\text{max}}/2, \eta_{\text{max}}/2) & \text{if } \text{Norm}(\eta_{\text{max}}/2, \eta_{\text{max}}/2) > 1 \\ 1 & \text{if } \text{Norm}(\eta_{\text{max}}/2, \eta_{\text{max}}/2) \leq 1 \end{cases} \quad (6)$$

We filter out the corresponding lineage solutions with perfect space robustness $S = N-2$, for that this condition is critical for embryogenesis and morphogenesis with cell-resolved accuracy [5,9,13]. Thus, proliferation rapidity and fate diversity are another two outputs of a lineage which can exist stably and reproducibly with perfect space robustness. To distinguish a specific lineage structure, we binarize the intervals between consecutive cell divisions $\{t_{i+1} - t_i\}$ and code a lineage structure with $\{\Delta t_i'\}$ ($1 \leq i \leq N-2$) in Eq. (7), where $\Delta t_i' = 0$ if the i^{th} interval belongs to a group of synchronous divisions, and $\Delta t_i' = 1$ if it belongs to two consecutive asynchronous divisions.

$$\{\Delta t'\} = [\Delta t_1', \Delta t_2', \dots, \Delta t_{N-2}'], \Delta t' = \begin{cases} 0 & \text{synchronous divisions} \\ 1 & \text{asynchronous divisions} \end{cases} \quad (7)$$

Some previous experimental measurements at second-level resolution revealed that the interval between AB and P1 divisions is around 2.0 ~ 2.5 minutes, which is between the two thresholds δ_s and δ_a obtained from 4- to 24-cell stages and doesn't affect the developmental accuracy, possibly due to its two-dimensional embryo structure [22]. For simplicity, we assume that the interval between 2- and 4-cell stages in *C. elegans* ($\Delta t_2'$) can be either 0 or 1.

RESULTS

Considering the huge parameter space, we first carry out 10^6 independent tests and obtain 148 non-identical solutions. For each solution, we perform perturbation on its sequence $\{\eta_i\}$ according to Eq. (8) (10^6 times for each), and finally find a total of 3533 solutions.

$$\eta_i' = \begin{cases} \text{Norm}(\eta_i, \eta_{\max}/2) & \text{if } \text{Norm}(\eta_i, \eta_{\max}/2) > 1 \\ 1 & \text{if } \text{Norm}(\eta_i, \eta_{\max}/2) \leq 1 \end{cases} \quad (8)$$

Both the amount of solutions and their extensive distribution in P - F space indicate considerable diversity and plasticity in nematode lineage design (P , 0.01221 ~ 0.01514; F , 1 ~ 13) [Figs. 3(a) and 4]. The *C. elegans* lineage is reproduced in both dimensions of fate specification and division order, which notably acquires high proliferation rapidity (pattern No. 2 in Fig. 3(a), within top 1%) [Figs. 1(b)-1(c) and 3].

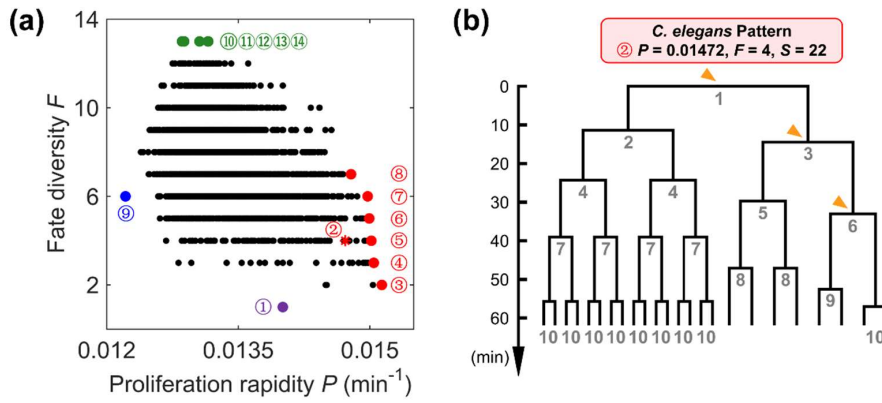


FIG. 3. Lineages solutions obtained from sampling simulation when $N = 24$. (a) Distribution of the 3533 non-identical solutions in P - F space; lineages with the lowest and highest fate diversity (No. 1 and No. 10 ~ 14), the lowest and highest proliferation rapidity (No. 9 and No. 3 ~ 8) are denoted with purple, green, blue and red points respectively; the *C. elegans* pattern is denoted by red asterisk (No. 2). (b) The *C. elegans* pattern; orange triangles denote the asymmetric divisions.

The lineages which proliferate fastest show common characteristics. The zygote must first divide asymmetrically and result in two fate-specific blastomeres; then the larger one undergoes symmetric and synchronous divisions, and produce identical descendants rapidly, while the asymmetric divisions occur in another blastomere (No. 2 ~ 6) [Figs. 4(b) and S1]. Alternatively, the asymmetric divisions can be programed in the larger blastomere to produce more cell types if the total time cost is hardly changed (No. 7 ~ 8), otherwise the time used to achieve the target cell number would be substantially lengthened (No. 9) [Figs. 4(a) and S1]. Note that, the difference of t_{N-1} between the slowest and fastest lineages can reach over 15 min, occupying 20% of the total duration from 1- to 24-cell stage. Intriguingly, the *C. elegans* pattern also obeys this rule and approaches the limit of proliferation rapidity, supporting that its extraordinary proliferation rapidity is attributed to the fine-designed lineage structure. It should be pointed out that, the lineages with high proliferation rapidity such as the *C. elegans* pattern depend little on the functions or parameters in the model (Supplemental Material 2 and Table S1). As many other related nematode species have a cell lineage pattern highly similar to that in *C. elegans* (e.g., *Caenorhabditis briggsae*, *Pellioditis marina*), they likely evolved under similar selective pressure which demands minimum time for development [23-25].

Fate diversity can be tuned extensively. Apparently, the lineage with the least cell types ($F = 1$) consists of only equal cleavage [Figs. 3(a) and 4(c)]; some can even produce 13 cell types by introducing 10 ~ 11 asymmetric divisions spread in the whole lineage, however, this excessive asymmetry results in lack of synchronous and rapid proliferation [Figs. 3(a) and 4(d)]. The final amount of cell types can range from 2 to 7 when its P value is larger than that in *C. elegans* pattern (No. 3 ~ 8). Those patterns probably exist in other kinds of nematode, for example, the pattern No. 6 has asymmetric division in a pair of sisters at 4-cell stage and subsequent significant asynchrony in their daughters, which is observed in a free-living marine nematode *Plectus sambesii* [26] [Fig. S1].

Proliferation rapidity can be increased by asymmetric division. The patterns No. 3 ~ 8 share common features that, 16 cells are generated by 4 rounds of highly synchronous divisions in a larger blastomere, while the other 8 cells are from the smaller blastomere which often undergoes asymmetric divisions [Fig. S1]. Their high proliferation rapidity is raised by the asymmetry in zygote division. Theoretically, cell division is completely synchronized in the fully symmetric case. At specific time points, the number of cells changes from n to $2n$. If, on the other hand, there is an asymmetry in the very beginning, i.e., $n/2$ cells have slightly greater volume than the other half, then this group would divide at an earlier time. So in between the embryo reaches $3n/2$ faster than the fully symmetric case.

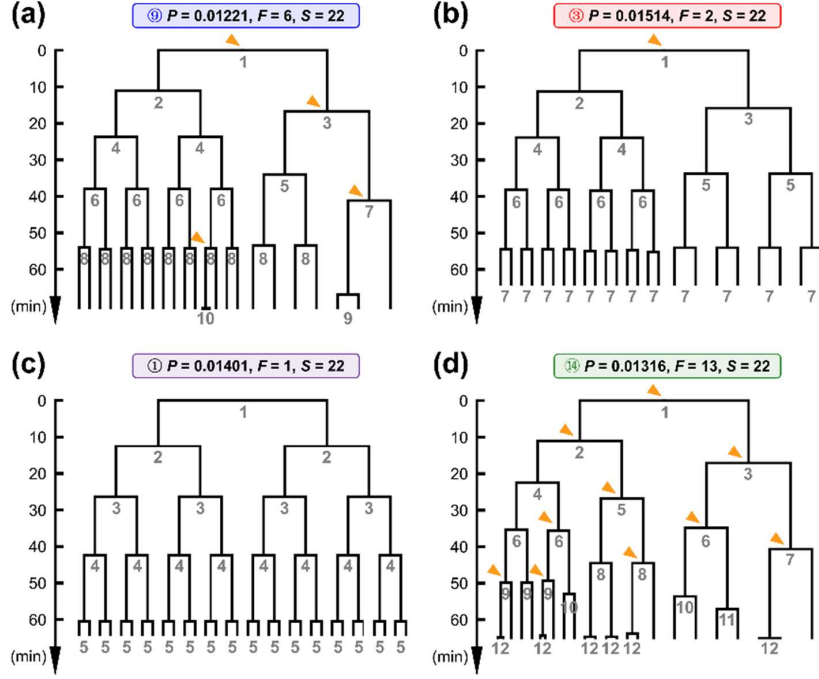


FIG. 4. Extreme lineages with (a) the lowest proliferation rapidity, (b) the highest proliferation rapidity, (c) the lowest fate diversity and (d) the highest fate diversity; orange triangles denote the asymmetric divisions.

DISCUSSION

Eutelic species has stereotypic developmental programs at single-cell level, especially for its cell lineage pattern. Why nematode embryo programs cell divisions with specific order and segregation ratio is elusive. In this work, a simple model is proposed to evaluate a lineage's performance in proliferation rapidity, fate diversity and space robustness, on the basis of two assumptions derived from *C. elegans* embryogenesis. The first is fate specification induced by asymmetric segregation of cell volume and its molecular contents; the second is the anti-correlation between cell cycle and cell volume. Given that space robustness is essential for developmental accuracy at cellular resolution, we simulate and filter out the lineages with perfect space robustness. The *C. elegans* pattern is well reproduced and shows an outstanding proliferation rapidity compared to the other solutions, suggesting a minimum time principle governing this system. This principle was also found in development of intestinal crypts, which leads to a sharp transition between symmetric and asymmetric stem cell divisions [19]. The restriction on time cost in development may be raised by competition among individuals, threat by predators and internal environment hostile to cell or embryo.

Since some solutions (e.g., patterns No. 3 ~ 8) also exhibit proliferation rapidity as high as the one in *C. elegans* pattern, other restrictions may exist as well. For instance, the pattern No. 5 has the same fate diversity to the *C. elegans* pattern ($F = 4$) and even higher proliferation rapidity [Fig. S1]. Why the *C. elegans* pattern is selected among those solutions still remains to be answered. One possibility is that, activating asymmetric divisions only on stem cells is the easiest to be realized and costs the least system resources such as genetic and proteomic programing [14].

The relationship between cell cycle and cell volume is regulated by dynamics of maternal-zygotic transition (MZT) [17-18]. Nematode species with different MZT dynamics have distinguishable relationships between cell cycle and cell volume, while some of them proliferates faster and faster over embryogenesis (e.g., *Acroboloides nanus*). To analyze the systems beyond *C. elegans*, one needs to revise the PFS model including both governing equations and system parameters, so as to recapture the fundamental interactions between different developmental properties.

This work provides a computational framework to simulate nematode lineage pattern, which can be further combined with developmental processes such as mechanical packing of cells and fate specification by cell-cell signaling [1,12-13,20-21]. The results provide new insights into the optimization principle in both embryogenesis and organogenesis [5,27], and lay a foundation for rational design of functional multicellular systems [28-29].

ACKNOWLEDGMENTS

We thank prof. Feng Liu, prof. Xiaojing Yang, Xiangyu Kuang and Jiajie Jiang for helpful discussion and comments. This work was supported by the Chinese Ministry of Science and Technology (Grant No. 2015CB910300), the National Natural Science Foundation of China (Grant No. 91430217), the Hong Kong Research Grants Council (Grants No. HKBU12100118, No. HKBU12100917, No. HKBU12123716, HKBU12301514) and the HKBU Interdisciplinary Research Cluster Fund. Computation was performed partly on the High-Performance Computing Platform at Peking University.

-
- [1] R. Fickentscher, P. Struntz and M. Weiss, *Biophys. J.* **105**, 1805 (2013).
 - [2] K. Khairy, W. Lemon, F. Amat and P. J. Keller, *Biophys. J.* **114**, 267 (2018).
 - [3] A. Mongera, P. Rowghanian, H. J. Gustafson, E. Shelton, D. A. Kealhofer, E. K. Carn, F. Serwane, A. A. Lucio, J. Giammona and O. Campàs, *Nature* **561**, 401 (2018).
 - [4] K. Ishihara, P. A. Nguyen, M. Wühr, A. C. Groen, C. M. Field and T. J. Mitchison, *Philos. Trans. R. Soc. B* **369**, 20130454 (2014).
 - [5] J. E. Sulston, E. Schierenberg, J. G. White and J. N. Thomson, *Dev. Biol.* **100**, 64 (1983).
 - [6] J. I. Murray, Z. Bao, T. J. Boyle and R. H. Waterston, *Nat. Protoc.* **1**, 1468 (2006).
 - [7] J. I. Murray, T. J. Boyle, E. Preston, D. Vafeados, B. Mericle, P. Weisdepp, Z. Zhao, Z. Bao, M. Boeck and R. H. Waterston, *Genome Res.* **22**, 1282 (2012).
 - [8] J. Cao, G. Guan, V. W. S. Ho, M. K. Wong, L. Y. Chan, C. Tang, Z. Zhao and H. Yan, *bioRxiv (preprint)*, 797688 (2019).
 - [9] G. Guan, M. K. Wong, V. W. S. Ho, X. An, L. Y. Chan, B. Tian, Z. Li, L. H. Tang, Z. Zhao and C. Tang, *bioRxiv (preprint)*, 776062 (2019).
 - [10] M. K. Wong, D. Guan, K. H. C. Ng, V. W. S. Ho, X. An, R. Li, X. Ren and Z. Zhao, *J. Biol. Chem.* **291**, 12501 (2016).
 - [11] J. Nance, J. Y. Lee and B. Goldstein. Gastrulation in *C. elegans* (September 26, 2005), WormBook, ed. The *C. elegans* Research Community, WormBook, <https://doi.org/10.1895/wormbook.1.23.1>.
 - [12] R. Fickentscher, P. Struntz P and M. Weiss, *Phys. Rev. Lett.* **117**, 188101 (2016).
 - [13] B. Tian, G. Guan, L. H. Tang and C. Tang, *Phys. Biol.* **17**, 026001 (2020).
 - [14] L. Hubatsch, F. Peglion, J. D. Reich, N. T. L. Rodrigues, N. Hirani, R. Illukkumbura and N. W. Goehring, *Nat. Phys.* **15**, 1078 (2019).
 - [15] A. Noatynska and M. Gotta, *Essays Biochem.* **53**, 1 (2012).
 - [16] Y. Arata, H. Takagi, Y. Sako and H. Sawa, *Front. Physiol.* **5**, 529 (2015).
 - [17] R. Fickentscher, S. W. Krauss and M. Weiss, *New J. Phys.* **20**, 113001 (2018).
 - [18] M. Laugsch and E. Schierenberg. *Int. J. Dev. Biol.* **48**, 655 (2004).
 - [19] S. Itzkovitz, I. C. Blat, T. Jacks, H. Clevers and A. V. Oudenaarden, *Cell* **148**, 608 (2012).
 - [20] C. J. Thorpe, A. Schlesinger, J. C. Carter and B. Bowerman, *Cell* **90**, 695 (1997).
 - [21] C. C. Mello, B. W. Draper and J. R. Prless, *Cell* **77**, 95-106 (1994).
 - [22] M. Brauchle, K. Baumer and P. Gönczy, *Curr. Biol.* **13**, 819 (2003).
 - [23] G. Guan G, M. K. Wong, L. Y. Chan, X. An, V. W. S. Ho, Z. Zhao and C. Tang. *ICBCB & ICBSIP 2020 (in press)* (2020).
 - [24] W. Houthoofd, K. Jacobsen, C. Mertens, S. Vangestel, A. Coomans and G. Borgonie, *Dev. Biol.* **258**, 57 (2003).
 - [25] W. Houthoofd and Borgonie G. *Nematology* **9**, 573 (2007).
 - [26] J. Schulze, W. Houthoofd, J. Uenk, S. Vangestel and E. Schierenberg, *EvoDevo* **3**, 13 (2012).
 - [27] J. E. Sulston, *Philos. Trans. R. Soc. B* **275**, 287 (1976).

- [28] S. Toda, L. R. Blauch, S. K. Y. Tang, L. Morsut and W. A. Lim, [Science](#) **361**, 156 (2018).
- [29] S. Kriegman, D. Blackiston, M. Levin and J. Bongard, [Proc. Natl. Acad. Sci. U.S.A.](#) **117**, 1853 (2020).
- [30] L. Chen, V. W. S. Ho, M. K. W. X. Huang, L. Y. Chan, H. C. K. Ng, X. Ren, H. Yan and Z. Zhao, [Genetics](#) **209**, 37 (2018)

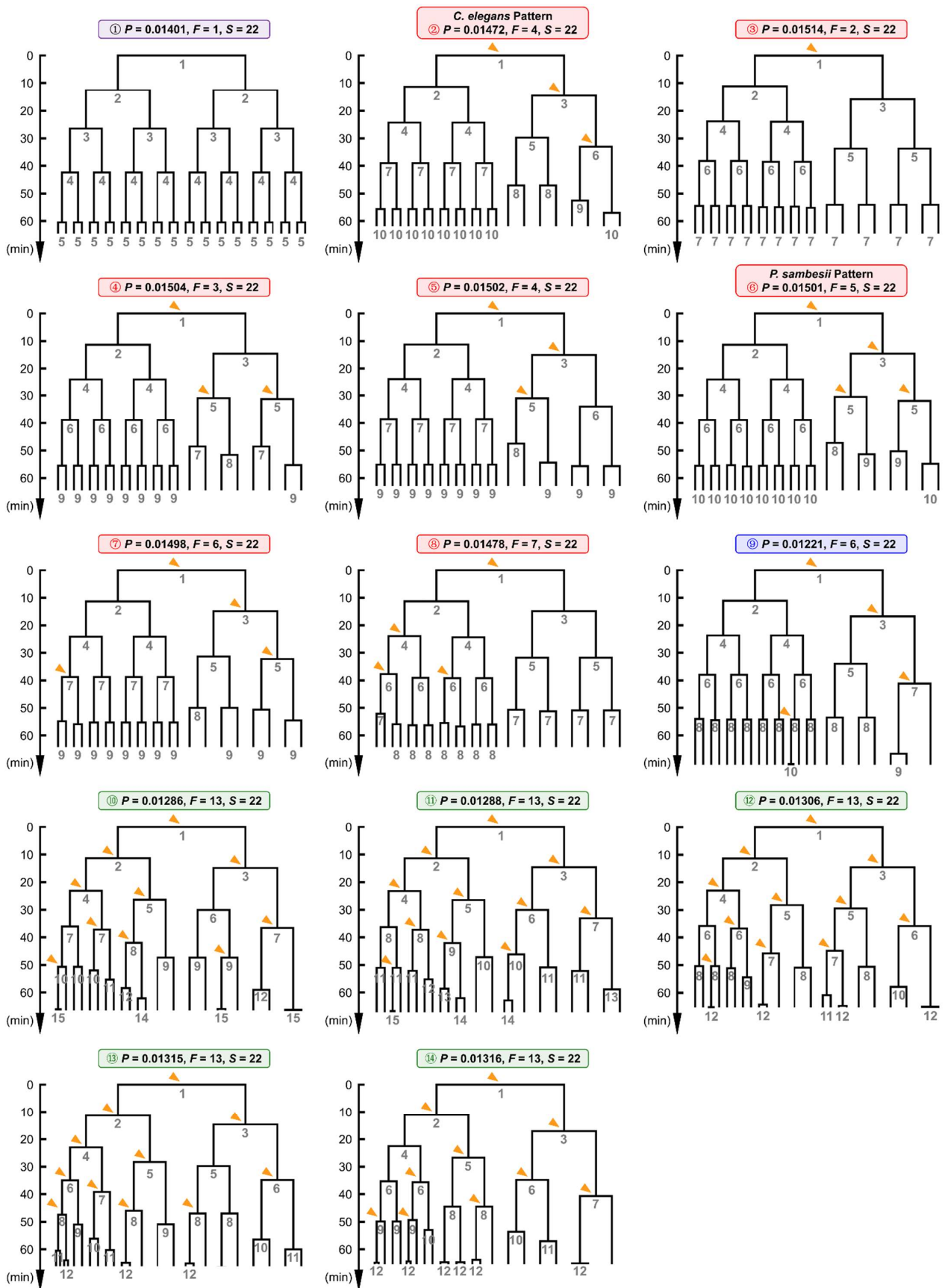


FIG. S1. Extreme lineage solutions highlighted in Fig. 3(a); orange triangles denote the asymmetric divisions.

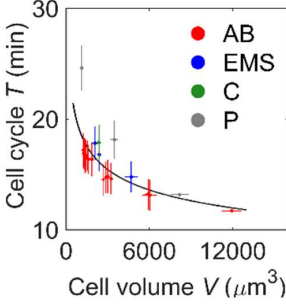
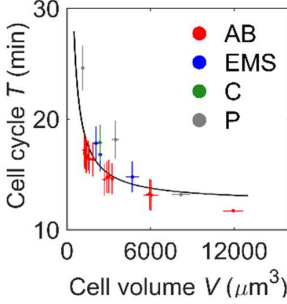
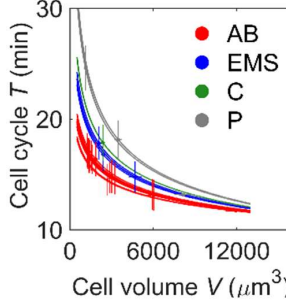
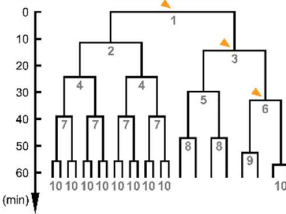
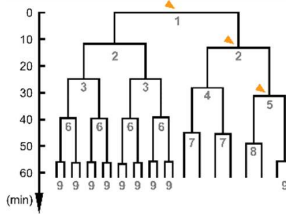
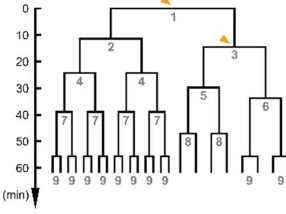
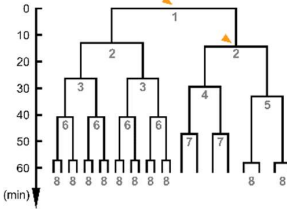
Supplemental Material 1

3D time-lapse images and quantitative tracing results of a wild-type embryo with GFP in cell nucleus and mCherry in cell membrane are provided (strain ZZY0535 [30]); developmental duration, 4- to 47-cell stage (60 time points); spatial resolution, 0.09 $\mu\text{m}/\text{pixel}$ in anterior-posterior and dorsal-ventral axes, 0.42 $\mu\text{m}/\text{pixel}$ in left-right axis; time resolution, 1.41 min/frame.

Supplemental Material 2

To verify if the high proliferation rapidity in *C. elegans* pattern depends on the specific form of Eq. (2), here we use three different functions and perform the same sampling simulation procedures as described in *METHODS* and *RESULTS* sections [Table S1]. The first is a general power law for all cells [16]; the second is a general inversely proportional function [12,17]; the third is power law functions which are fitted onto each cell with constant T_1 and variable β' . Proliferation rapidity in *C. elegans* pattern (asymmetry in P0, P1 and P2 divisions) and its subtype (asymmetry only in P0 and P1 divisions) is calculated, which is always ranked within top 1%.

Table S1. Lineage simulation using different functions for the anti-correlation between cell cycle and cell volume.

| Function | $T = T_1(V/V_1)^{-\beta}$ | $T = \tau_M + \alpha/V$ | $T = T_1(V/V_1)^{-\beta'}$ |
|---|---|--|---|
| Parameter setting | $T_1 = 10.90 \text{ min}$ $\beta = 0.1831$ | $\tau_M = 12.48 \text{ min}$ $\alpha = 7731 \mu\text{m}^3$ | $T_1 = 10.90 \text{ min}$ β' is determined by experiments for each cell. |
| R^2 | 0.6317 | 0.5425 | 1 |
| Fitting results |  |  |  |
| Solutions in the first round of sampling | 148 | 228 | 63 |
| Solutions in the second round of sampling | 3533 | 5975 | 1607 |
| If there's a <i>C. elegans</i> pattern? |  | / |  |
| If there's a subtype pattern? |  |  | / |
| Ranking of the patterns in proliferation rapidity | I. 31/3533 $\approx 0.88\%$ II. 5/3533 $\approx 0.14\%$ | II. 26/5975 $\approx 0.44\%$ | I. 2/1607 $\approx 0.12\%$ |

Solution distribution
(red asterisk, *C. elegans*
pattern; red circle,
subtype)

